Clinical Investigation

Magnetic Resonance Imaging in Pediatric Pulmonary Hypertension

Ayhan Pektas, MD
Rana Olgunturk, MD
Ayhan Cevik, MD
Semiha Terlemez, MD
Emre Kacar, MD
Yusuf Ali Oner, MD

Key words: *Aorta, thoracic/radiography; cardiac catheterization; child; hypertension, pulmonary/diagnosis/physiopathology; magnetic resonance imaging; pulmonary artery/radiography; retrospective studies; ROC curve; sensitivity and specificity*

From: *Department of Pediatric Cardiology (Drs. Cevik, Olgunturk, Pektas, and Terlemez), Gazi University Medical Faculty Hospital, 06560 Ankara; and Department of Radiology (Drs. Kacar and Oner), Gazi University Medical Faculty Hospital, 06590 Ankara; Turkey*

Dr. Pektas is now at the Department of Pediatric Cardiology and Dr. Kacar at the Department of Radiology, Afyon Kocatepe University Medical Faculty Hospital, Afyonkarahisar, Turkey. Dr. Cevik is now at the Department of Pediatric Cardiology, Sisli Florence Nightingale Hospital, Istanbul, Turkey. Dr. Terlemez is now at the Department of Pediatric Cardiology, Adnan Menderes University Medical Faculty Hospital, Aydin, Turkey.

Address for reprints:
Ayhan Pektas, MD, Selcuklu Mah. Adnan Kahveci Cad. No: 16/2, 03200 Afyonkarahisar, Turkey

E-mail:
drayhanpektas@hotmail.com

The present study aims to determine the efficacy and reliability of cardiovascular magnetic resonance imaging in establishing the diagnosis and prognosis of pulmonary hypertension in children.

This is a retrospective comparison of 25 children with pulmonary hypertension and a control group comprising 19 healthy children. The diagnosis of pulmonary hypertension was made when the mean pulmonary artery pressure was ≥25 mmHg by catheter angiography.

The children with pulmonary hypertension had significantly lower body mass indices than did the healthy children (P=0.048). In addition, the children with pulmonary hypertension had significantly larger main pulmonary artery diameters and ascending aortic diameters (both P=0.001) but statistically similar ratios of main pulmonary artery diameter-to-ascending aortic diameter. If the main pulmonary artery diameter was ≥25 mm, pediatric pulmonary hypertension was diagnosed with 72% sensitivity and 84% specificity. In the event that the ratio of main pulmonary artery diameter-to-ascending aorta diameter was ≥1, pediatric pulmonary hypertension was diagnosed with 60% sensitivity and 53% specificity. When compared with children who had New York Heart Association functional class II pulmonary hypertension, the children with functional class III pulmonary hypertension had significantly larger main (P=0.046), right (P=0.036), and left (P=0.003) pulmonary arteries.

Cardiovascular magnetic resonance imaging is useful in the diagnosis of children with pulmonary hypertension. Pediatric pulmonary hypertension can be diagnosed with high sensitivity and specificity when the main pulmonary artery diameter measures ≥25 mm.
(Tex Heart Inst J 2015;42(3):209-15)

Pulmonary hypertension (PH) is diagnosed when the resting mean pulmonary artery (PA) pressure is ≥25 mmHg. It has been hypothesized that abnormal hemodynamic effects of various stimuli cause PH, which in turn progressively leads to heart failure and eventually to death. This clinical entity can be either idiopathic or secondary to various clinical conditions.[1-3]

Childhood PH is especially associated with congenital heart disease in children. Although childhood PH is usually related to acyanotic heart disease, it can also occur in children with cyanotic heart defects. Angiography is the gold standard for the diagnosis and follow-up of PH. This diagnostic tool, in experienced hands, has substantially lowered the morbidity and mortality rates associated with childhood PH. However, angiography is an invasive procedure that can give rise to severe complications. Therefore, easily available and noninvasive imaging methods such as echocardiography, computed tomography, and magnetic resonance imaging (MRI) have been adopted for the clinical consideration of this disease.[1-5]

Among these noninvasive techniques, MRI is of pronounced importance, because it enables the visual evaluation of accompanying heart defects, pulmonary parenchyma, and the pulmonary vasculature in the clinical study of PH patients. Combining contiguous bright-blood cine MRI slices (8 mm thick), acquired in short-axis orientation, makes possible the calculation of end-systolic and end-diastolic ventricular volumes, ejection fractions, and myocardial mass. The high degree of accuracy and reproducibility of these derived measures facilitates the evaluation of disease severity and

This work was supported by the Scientific Research Projects Board of Gazi University Medical Faculty (grant no. SBE 01/2011-71).

early-stage changes in cardiac structure and function.[6-8] Moreover, it has been proposed that the enlargement of main PA diameter and the subsequent increase in the ratio of main PA diameter-to-ascending aorta diameter might indicate the pathologic increment in PA pressure.

The present study aims to determine the efficacy and reliability of MRI in the establishment of PH diagnosis and prognosis in children.

Patients and Methods

The present study was approved by our local ethics committee (decision no: 125/21.03.2012). All MRI measurements were made by 2 experienced radiologists (AYO and EK). Intra- and interobserver variations were evaluated by means of the Bland-Altman method.[9]

This is a retrospective review of 44 children who were consecutively evaluated at the department of pediatric cardiology at Gazi University Medical Faculty Hospital from January 2001 through March 2012. The study group consisted of 25 children with PH and 19 healthy children. The diagnosis of PH was made when mean PA pressure was ≥25 mmHg by catheter angiography. In order to determine the severity of the disease for each child diagnosed with PH, the New York Heart Association (NYHA) functional classification system was used. Data related to demographic features, clinical characteristics, catheter angiographic results, MRI findings, and serum concentrations of brain natriuretic peptide (BNP) were evaluated. Body mass index was calculated in accordance with the following formula:

Body mass index (kg/m^2) = body weight (kg) / height^2 (m^2).

Angiography. In accordance with the standard techniques, angiography was performed by using a Swan-Ganz catheter. Right atrial pressure, PA pressures (systolic, diastolic, and mean), pulmonary flow rate (Q p), systemic flow rate (Qs), the Q p/Qs, pulmonary vascular resistance (PVR), systemic vascular resistances (SVR), and the PVR/SVR ratio were recorded. Pulmonary and systemic flow rates were both computed by application of the Fick principle, on the basis of oxygen consumption in accordance with age, sex, and heart rate. The value of PVR in Wood units was calculated according to the following equation:

Pulmonary vascular resistance = [mean PA pressure – PA occlusion pressure (mmHg)] × 80 / cardiac output.

Magnetic Resonance Imaging. Each child with PH underwent MRI within 3 months of the angiographic procedure. For image acquisition, a 32-channel 1.5-Tesla whole-body MAGNETOM® Avanto magnetic resonance scanner (Siemens Medical Solutions USA, Inc.; Mountain View, Calif) was used: maximum gradient 45 mT/m amplitude; slew rate, 200 (mTm^{-1}) / ms; 17-element matrix coil (8 anterior and 9 posterior) activated for data collection, and 3-electrode electrocardiographic (ECG) leads applied for ECG gating. Before the examination, the patients were laid supine on the imaging table and were entered head-first into the magnetic field. The typical scan time of the 2-dimensional steady-state free-precession was 4 to 6 s per slice, and 30 to 40 slices of 8 mm were obtained without gaps, to cover the thorax. Operators sampled data in a linear fashion by using a navigator-gating technique with a 6- to 8-mm window; right diaphragmatic movement was tracked via motion-adapted tracking, or a respiratory gating technique (using a belt sensor) suppressed respiratory motion artifacts. Noncontrast-enhanced 3-dimensional (3D) magnetic resonance aortograms of the thorax were obtained with use of a cardiac-gated, respiratory-compensated, 3D k-space segmented, T1-weighted, gradient-echo imaging sequence. Zero-filling interpolation was used to reduce the partial volume effect in the slice direction. Spectrally selective fat-suppression and T2-preparation pulses, which consisted of 2 radiofrequency pulses in a preparation time of 50 ms, suppressed the background signals from mediastinum and myocardium. Typically, acquisitions used 1- to 2-mm in-plane resolution (8-mm section thickness) with tricuspid regurgitation values of 2 ms to 3.2 ms, tricuspid valve E velocity values of 1.3 ms (opposed phase) to 2.5 ms (in phase), and a flip angle of 8°. The images covered a 256 × 256-mm 2° field of view, with a base resolution of 128 to 256 data samples.

A 3D model of the aorta and the PA was constructed by combining the diameters measured

- at the level of the diaphragm (corresponding to the diameter of the descending aorta),
- at the level of the right PA within the axial plane (corresponding to the diameter of the ascending aorta),
- at the level of the pulmonary bifurcation (corresponding to the diameter of the main PA),
- at the point between the left common carotid and left subclavian arteries (corresponding to the diameter of the mid-aortic arch), and
- at the point between the pulmonary bifurcation and the offspring of the lobe branches (corresponding to the diameters of the right and left PAs).

Statistical Analysis

Collected data were analyzed by use of SPSS version 18.0 (IBM Corporation; Armonk, NY) on computerized media. The Shapiro-Wilk test was used to test the distribution of continuous variables. Continuous variables were expressed as either mean ± SD or as median (range, 25th–75th percentile), and categorical variables

were denoted as numbers or percentages where appropriate. The Student *t* test and the Mann-Whitney U test were used to compare, retrospectively, the continuous and categorical variables of 2 independent groups. The Pearson correlation test was used to specify the relationships among variables. Receiver operating characteristic (ROC) curves were drawn to manifest the predictive power of radiologic values for the diagnosis of PH at pediatric age. Two-tailed *P* values of less than 0.05 were considered statistically significant.

Results

Demographic Characteristics, Clinical Features, and Radiologic Findings

In Table I, the demographic characteristics of the 25 children diagnosed with PH are compared with those of the 19 healthy children. The children with PH had significantly shorter body height ($P=0.013$), as well as significantly lower body weight ($P=0.022$) and body mass index ($P=0.048$).

Table II summarizes the broad clinical features of the 25 children with PH. More specifically, ventricular septal defect was present in 8 children (32%), transposition of the great arteries in 3 (12%), double-outlet right ventricle in 3 (12%), atrial septal defect in 2 (8%), truncus arteriosus in 2 (8%), dilated cardiomyopathy in 2 (8%), and aortopulmonary window in 1 child (4%) with PH. Meanwhile, 3 children (12%) had idiopathic PH and 1 child (4%) had thromboembolic PH.

Table III compares the radiologic findings for the 25 children with PH with those for the 19 healthy control subjects. When compared with the healthy children, the children with PH had significantly larger diameters of the main PA diameter and the ascending aorta (both $P=0.001$) but statistically similar ratios of main PA diameter-to-ascending aorta diameter.

Figure 1 illustrates the ROC curves of 2 radiologic values for the prediction of PH in children. The area under the ROC curve for main PA diameter (see 1A) is computed as 0.883 ± 0.052, whereas the area under ROC curve for the ratio of main PA diameter-to-ascending aorta diameter (see 1B) is calculated as 0.642 ± 0.03.

Table IV lists the results of ROC analysis. If the main PA diameter was ≥25 mm, pediatric PH was diagnosed with 72% sensitivity and 84% specificity. In the event that the main PA diameter was ≥35 mm, the sensitivity was reduced to 36% and the specificity was increased to 95%. If the ratio of the main PA diameter-to-ascending aorta diameter was ≥1, pediatric PH was diagnosed with 60% sensitivity and 53% specificity. When the ratio of main PA diameter-to-ascending aorta diameter was ≥1.45, the sensitivity was reduced to 44% and the specificity was increased to 90%.

For the first radiologist (AYO), the mean difference between the 2 measurements corresponded to –0.029 (95% confidence interval [CI], –0.035 to –0.020), whereas for the 2nd radiologist (EK), the mean difference between the 2 measurements was computed to be –0.038 (95% CI, –0.056 to –0.011). The limits of agreement were from –0.16 to 0.28 for AYO and from –0.24 to 0.33 for EK. When the interobserver variation was evaluated in 34 cases, the mean difference between the 2 observers was –0.034 (95% CI, –0.049 to –0.018). The limits of agreement were from –0.22 to 0.30.

Correlation between Biochemical and Hemodynamic Values

There was a significant and positive correlation between serum BNP concentration and the diameter of the right PA ($r=0.472$, $P=0.023$). Moreover, a significant and positive correlation was detected between serum BNP levels and PVR values ($r=0.59$, $P=0.026$). When compared with children who were in NYHA functional class II PH, the class III children had significantly larger diameters of the main PA (28.6 ± 9.6 vs 36.8 ± 8.8 mm; $P=0.046$), the right PA (14.7 ± 4.5 vs 20.1 ± 6.9 mm; $P=0.036$), and the left PA (12.8 ± 5.6 vs 20.8 ± 5.9 mm; $P=0.003$).

Discussion

As a noninvasive technique, MRI is useful in the clinical evaluation of the patients whose clinical signs and symptoms create a high degree of suspicion for PH. This

TABLE I. Demographic Characteristics of the Study Cohort

Variable	**Pulmonary Hypertension Pts.** (n=25)	**Healthy Control Subjects** (n=19)	***P* Value**
Age (yr)	12.6 ± 4.6	13.3 ± 1.7	0.532
Male	14 (56)	9 (47.4)	0.761
Body height (m)	1.42 ± 0.22	1.56 ± 0.1	0.013
Body weight (kg)	38.8 ± 14.8	51 ± 9.3	0.022
Body mass index (kg/m^2)	18.49 ± 4	20.73 ± 2.33	0.048

Data are expressed as mean ± SD or as number and percentage. $P<0.05$ was considered statistically significant.

imaging technique enables the study not only of cardiac morphology (such as ventricular dimension, volume, and wall thickness), but of the morphology and distensibility of the PA.[10,11]

TABLE II. Clinical Features of the 25 Children with Pulmonary Hypertension

Variable	Value
PA pressure (mmHg)	71.8 ± 18.4
Systolic PA pressure (mmHg)	100 ± 22.1
Diastolic PA pressure (mmHg)	48.8 ± 20.3
Pulmonary vascular resistance (Wood units)	20.4 ± 16.2
Brain natriuretic peptide (pg/mL)	1,896.6 ± 1,212.6
NYHA functional class	
II	12 (48)
III	13 (52)

NYHA = New York Heart Association; PA = pulmonary artery

Data are presented as mean ± SD or as number and percentage.

Investigators in previously published studies have shown the ability of cardiovascular MRI to distinguish PH patients from healthy subjects. These studies have indicated that PA pressure correlates with radiologic values in such a manner that patients with PH can be identified on the basis of PA dilation. However, these findings arise from contradictory data obtained from small-scale studies that recruit adult patients exclusively. To the best of our knowledge, ours is the first study to evaluate the efficacy and reliability of cardiovascular MRI findings in pediatric PH patients.

Nikolaou and colleagues[12] used both fast-perfusion MRI and high-resolution MRI angiography to evaluate patients with idiopathic PH and chronic thromboembolic PH. Dynamic perfusion images and reconstructed 3D magnetic resonance angiograms were examined for occlusive and nonocclusive alterations in the PAs, such as perfusion defects, caliber irregularities, and intravascular thrombi. These 2 MRI-derived techniques were not only compatible with each other but had, in combination, a sensitivity of 90%.

Velocity-encoded phase-contrast MRI has been used in the study of hemodynamic changes associated with PH. When patients with PH were compared with healthy control subjects,[13] PA mean peak flow velocity,

TABLE III. Radiologic Findings in the Study Cohort

Vessel Diameter	Pulmonary Hypertension Pts. (n=25)	Healthy Control Subjects (n=19)	*P* Value
Main PA diameter (mm)	32.4 ± 9.6	19.5 ± 7.7	0.001
Right PA diameter (mm)	17.3 ± 6.3	14.6 ± 1.6	0.065
Left PA diameter (mm)	17 ± 7	15.2 ± 1.6	0.231
Ascending aortic diameter (mm)	25.5 ± 8.7	17.8 ± 5	0.001
Descending aortic diameter (mm)	16.4 ± 5.7	15.2 ± 1.1	0.425
Main PA-to-ascending aorta diameter (mm)	1.4 ± 0.9	1.1 ± 0.2	0.08

PA = pulmonary artery; Pts. = patients

Data are expressed as mean ± SD. P <0.05 was considered statistically significant.

TABLE IV. Results of Receiver Operating Characteristic Analysis

Vessel Diameter	Sensitivity (%)	Specificity (%)	Positive Predictive Value (%)	Negative Predictive Value (%)
Main PA diameter ≥25 mm	72.0	84.2	85.7	69.6
Main PA diameter ≥29 mm	64.0	89.5	88.9	65.4
Main PA diameter ≥35 mm	36.0	94.7	90.0	75.0
Main PA-to-ascending aortic diameter ≥1	60.0	52.6	62.5	50.0
Main PA-to-ascending aortic diameter ≥1.45	44.0	89.5	84.6	54.8

PA = pulmonary artery

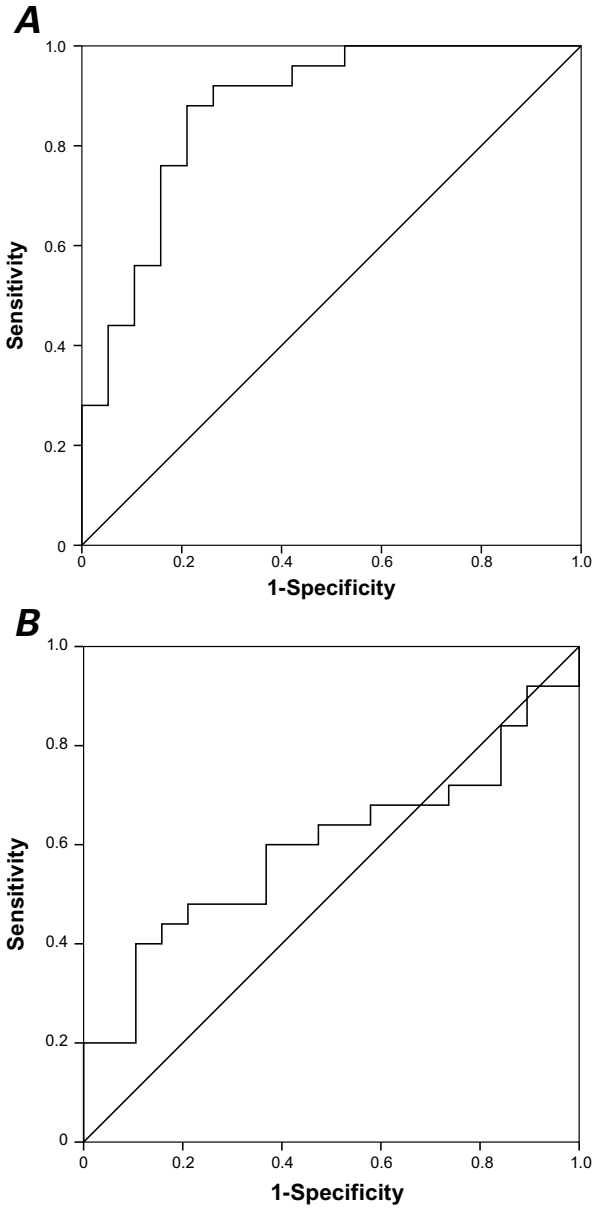

Fig. 1 *Receiver operating characteristic curves for* ***A****) main pulmonary artery diameter (area under the curve, 0.883 ± 0.052) and* ***B****) the ratio of pulmonary artery diameter to ascending aorta diameter (area under the curve, 0.642 ± 0.03).*

blood flow, and distensibility were significantly lower in the PH patients ($P=0.002$, $P=0.002$, and $P=0.008$, respectively). That study also documented that, among PH patients, the time to achieve peak PA velocity was reduced and the velocity increase gradient was steeper.[13]

Laffon and associates[14] developed a computerized algorithm for estimating mean PA pressure on the basis of an MRI evaluation of such physical values as PA cross-sectional area and blood-flow velocity. This algorithm was also adjusted for patient-specific biophysical values, including height, weight, and heart rate. When the resultant algorithm was applied to a series of 31 patients undergoing right-sided heart catheterization, catheterization-derived values correlated strongly with the mean PA pressure (which had been calculated on the basis of the MRI-derived values) ($r=0.92$).

Investigators in a 2007 study[15] examined 59 PH patients who underwent both right-sided heart catheterization and phase-contrast MRI. The average PA velocity had the best correlation with mean PA pressure, systolic PA pressure, and PVR index. It was then suggested that this strong correlation might enable the noninvasive diagnosis of PH.

In contrast with these generally positive results, Roeleveld and colleagues[16] found poor correlation between catheter-derived mean PA pressure and 5 different MRI-derived measures, including pulmonary vascular index, acceleration time (defined as time from onset of PA forward flow to maximum velocity), the ratio between acceleration time and ejection time, and the Laffon algorithm discussed previously. The only significant correlation between catheter-derived mean PA pressure and MRI-derived values was for ventricular mass index ($r=0.56$, $P=0.001$). However, there was a false-negative rate of 20% if a cutoff value of >0.6 was adopted for ventricular mass index. It was concluded, therefore, that MRI-derived measures—although possibly sufficient for screening and differential diagnosis—could not replace right-sided heart catheterization in confirming a PH diagnosis.

Another study, which compared fast-gradient echocardiographic phase-contrast MRI with radionuclide lung perfusion in 12 pediatric cases of suspected unilateral PA branch stenosis, concluded that these 2 methods were equally effective in evaluating differential blood flow in the pulmonary branches.[17]

A conclusion of our present study is that childhood PH can be diagnosed with 72% sensitivity and 84% specificity in the event that the PA diameter is ≥25 mm. Few studies have focused on the MRI measurement of major-vessel diameters. In one such study, by Kutty and co-authors,[18] the mean diameter of the main PA was given as 23 mm and the mean body surface area as 1.4 m^2, in healthy adolescents with a mean age of approximately 14 years. Investigators in another study found the mean diameter of the main PA to be 24 ± 2.8 mm in 26 adults (age range, 19–46 yr) who had normal thoracic computed tomographic results and normal PA pressures.[19] It would then be rational to accept 25 mm as the cutoff value for main PA diameters in the diagnosis of PH in children.

In this study, we were unable to detect a significant difference between the PA-to-ascending aorta ratios of the healthy and PH-affected children. Moreover, the sensitivity and specificity were reduced to 60% and 53%, respectively, if the ratio of main PA diameter-to-ascending aorta diameter was ≥1. These findings might arise from the possibility that the PA and ascending

aorta diameters broaden simultaneously—in parallel both with advancing age and with underlying disease.

On the other hand, there were no strong correlations between hemodynamic values and radiologic measurements in pediatric PH patients. This discrepancy might be due to the variations in diagnostic criteria for PH, to the clinical characteristics of reviewed patients (especially in regard to age and underlying congenital heart disease), and to cohort size. An advantage of the present study is the enrollment of radiologic data by means of ECG-triggered MRI. In the event that ECG-triggered MRI is not performed, heartbeat cycle and respiratory movements can interfere with the radiologic measurements.[8] In order to minimize the curative effects of medical treatment upon the pulmonary vascular bed, each child with PH had MRI within 3 months of the catheter angiographic procedure.

A case-control cohort study of 3,171 adults revealed a positive correlation between mean PA diameter and body height.[20] Similarly, a significant linear correlation was found between the diameter of the orifice of the pulmonary trunk and body height or weight in 35 healthy children.[21] Like correlations were found for the measurements of the aortic orifice and body height or weight in the same cohort. Moreover, Akay and associates[22] evaluated 133 pediatric patients and indicated a positive correlation between patient age and the diameters of the ascending aorta, descending aorta, and PAs. Our findings show that the diameters of the main PA and the ascending aorta were significantly larger, despite significantly lower body weights and heights of the pediatric PH patients. In other words, the detection of significantly large PA and aorta diameters in children of small constitution would suggest a diagnosis of PH.

The power of the present study is limited by several factors. First, this study reviews a relatively small cohort. Second, the study cohort generally includes children who were diagnosed with PH secondary to congenital heart diseases. Both factors might impair the application of the acquired data to all children with PH, whether the underlying mechanism for PH is idiopathic, thromboembolic, or a congenital heart defect. The 3rd factor is the lack of subgroup analysis with respect to the diameter of the ascending aorta. In fact, the width of the ascending aorta might be increased in the presence of aortic valve disease. The 4th factor is the relatively low predictive power of ROC analysis. In addition, MRI use in children is limited by such factors as variations in spatial resolution, difficulty in breath-holding, and the need for anesthesia. In general, the paucity of data about confounding factors could have damaged the trustworthiness of calculations that relied on ascending aorta diameter.

In conclusion, the diagnosis of childhood PH can be made with relatively higher sensitivity and specificity when the PA diameter is ≥25 mm. Alterations in MRI findings can be used as well, to form a prognosis of PH in children. However, further research is warranted to determine the efficacy and reliability of MRI in pediatric PH patients.

References

1. Galie N, Hoeper MM, Humbert M, Torbicki A, Vachiery JL, Barbera JA, et al. Guidelines for the diagnosis and treatment of pulmonary hypertension: the Task Force for the Diagnosis and Treatment of Pulmonary Hypertension of the European Society of Cardiology (ESC) and the European Respiratory Society (ERS), endorsed by the International Society of Heart and Lung Transplantation (ISHLT) [published erratum appears in Eur Heart J 2011;32(8):926]. Eur Heart J 2009;30 (20):2493-537.
2. Cerro MJ, Abman S, Diaz G, Freudenthal AH, Freudenthal F, Harikrishnan S, et al. A consensus approach to the classification of pediatric pulmonary hypertensive vascular disease: report from the PVRI Pediatric Taskforce, Panama 2011. Pulm Circ 2011;1(2):286-98.
3. Simonneau G, Robbins IM, Beghetti M, Channick RN, Delcroix M, Denton CP, et al. Updated clinical classification of pulmonary hypertension. J Am Coll Cardiol 2009;54(1 Suppl):S43-54.
4. Haworth SG. The management of children with congenital heart disease. In: Beghetti M, Barst RJ, Naeije R, Rubin LJ, editors. Pulmonary arterial hypertension related to congenital heart disease. New York: Elsevier; 2006. p. 129-41.
5. Hoeper MM, Lee SH, Voswinckel R, Palazzini M, Jais X, Marinelli A, et al. Complications of right heart catheterization procedures in patients with pulmonary hypertension in experienced centers. J Am Coll Cardiol 2006;48(12):2546-52.
6. Torbicki A. Cardiac magnetic resonance in pulmonary arterial hypertension: a step in the right direction. Eur Heart J 2007;28(10):1187-9.
7. Benza R, Biederman R, Murali S, Gupta H. Role of cardiac magnetic resonance imaging in the management of patients with pulmonary arterial hypertension. J Am Coll Cardiol 2008;52(21):1683-92.
8. Amano Y, Takahama K, Kumita S. Noncontrast-enhanced three-dimensional magnetic resonance aortography of the thorax at 3.0 T using respiratory-compensated T1-weighted k-space segmented gradient-echo imaging with radial data sampling: preliminary study. Invest Radiol 2009;44(9):548-52.
9. Bland JM, Altman DG. Applying the right statistics: analyses of measurement studies. Ultrasound Obstet Gynecol 2003;22 (1):859-93.
10. Rathi VK, Mikolich B, Patel M, Doyle M, Yamrozik J, Biederman RW. Coronary artery fistula; non-invasive diagnosis by cardiovascular magnetic resonance imaging. J Cardiovasc Magn Reson 2005;7(4):723-5.
11. Junqueira FP, Lima CM, Coutinho AC Jr, Parente DB, Bittencourt LK, Bessa LG, et al. Pulmonary arterial hypertension: an imaging review comparing MR pulmonary angiography and perfusion with multidetector CT angiography. Br J Radiol 2012;85(1019):1446-56.
12. Nikolaou K, Schoenberg SO, Attenberger U, Scheidler J, Dietrich O, Kuehn B, et al. Pulmonary arterial hypertension: diagnosis with fast perfusion MR imaging and high-spatial-resolution MR angiography--preliminary experience. Radiology 2005;236(2):694-703.
13. Ley S, Mereles D, Puderbach M, Gruenig E, Schock H, Eichinger M, et al. Value of MR phase-contrast flow measurements for functional assessment of pulmonary arterial hypertension. Eur Radiol 2007;17(7):1892-7.

14. Laffon E, Vallet C, Bernard V, Montaudon M, Ducassou D, Laurent F, Marthan R. A computed method for noninvasive MRI assessment of pulmonary arterial hypertension. J Appl Physiol 2004;96(2):463-8.
15. Sanz J, Kuschnir P, Rius T, Salguero R, Sulica R, Einstein AJ, et al. Pulmonary arterial hypertension: noninvasive detection with phase-contrast MR imaging. Radiology 2007;243(1):70-9.
16. Roeleveld RJ, Marcus JT, Boonstra A, Postmus PE, Marques KM, Bronzwaer JG, Vonk-Noordegraaf A. A comparison of noninvasive MRI-based methods of estimating pulmonary artery pressure in pulmonary hypertension. J Magn Reson Imaging 2005;22(1):67-72.
17. Sridharan S, Derrick G, Deanfield J, Taylor AM. Assessment of differential branch pulmonary blood flow: a comparative study of phase contrast magnetic resonance imaging and radionuclide lung perfusion imaging. Heart 2006;92(7):963-8.
18. Kutty S, Kuehne T, Gribben P, Reed E, Li L, Danford DA, et al. Ascending aortic and main pulmonary artery areas derived from cardiovascular magnetic resonance as reference values for normal subjects and repaired tetralogy of Fallot. Circ Cardiovasc Imaging 2012;5(5):644-51.
19. Bozlar U, Ors F, Deniz O, Uzun M, Gumus S, Ugurel MS, et al. Pulmonary artery diameters measured by multidetector-row computed tomography in healthy adults. Acta Radiol 2007;48(10):1086-91.
20. Truong QA, Massaro JM, Rogers IS, Mahabadi AA, Kriegel MF, Fox CS, et al. Reference values for normal pulmonary artery dimensions by noncontrast cardiac computed tomography: the Framingham Heart Study. Circ Cardiovasc Imaging 2012;5(1):147-54.
21. Robida A. Diameters of the orifices of the aorta and pulmonary trunk in normal children--an angiocardiographic study. Int J Cardiol 1987;14(3):319-25.
22. Akay HO, Ozmen CA, Bayrak AH, Senturk S, Katar S, Nazaroglu H, Taskesen M. Diameters of normal thoracic vascular structures in pediatric patients. Surg Radiol Anat 2009; 31(10):801-7.